

# **A Case Study Report on Prediction of Future Land Cover Changes of Ben Cat District, Vietnam using QGIS MOLUSCE Plugin**

Innovative Tools to Support the Design and Monitoring of NBS and GHG Emission Reduction Projects (LoA/RAP/2023/48)

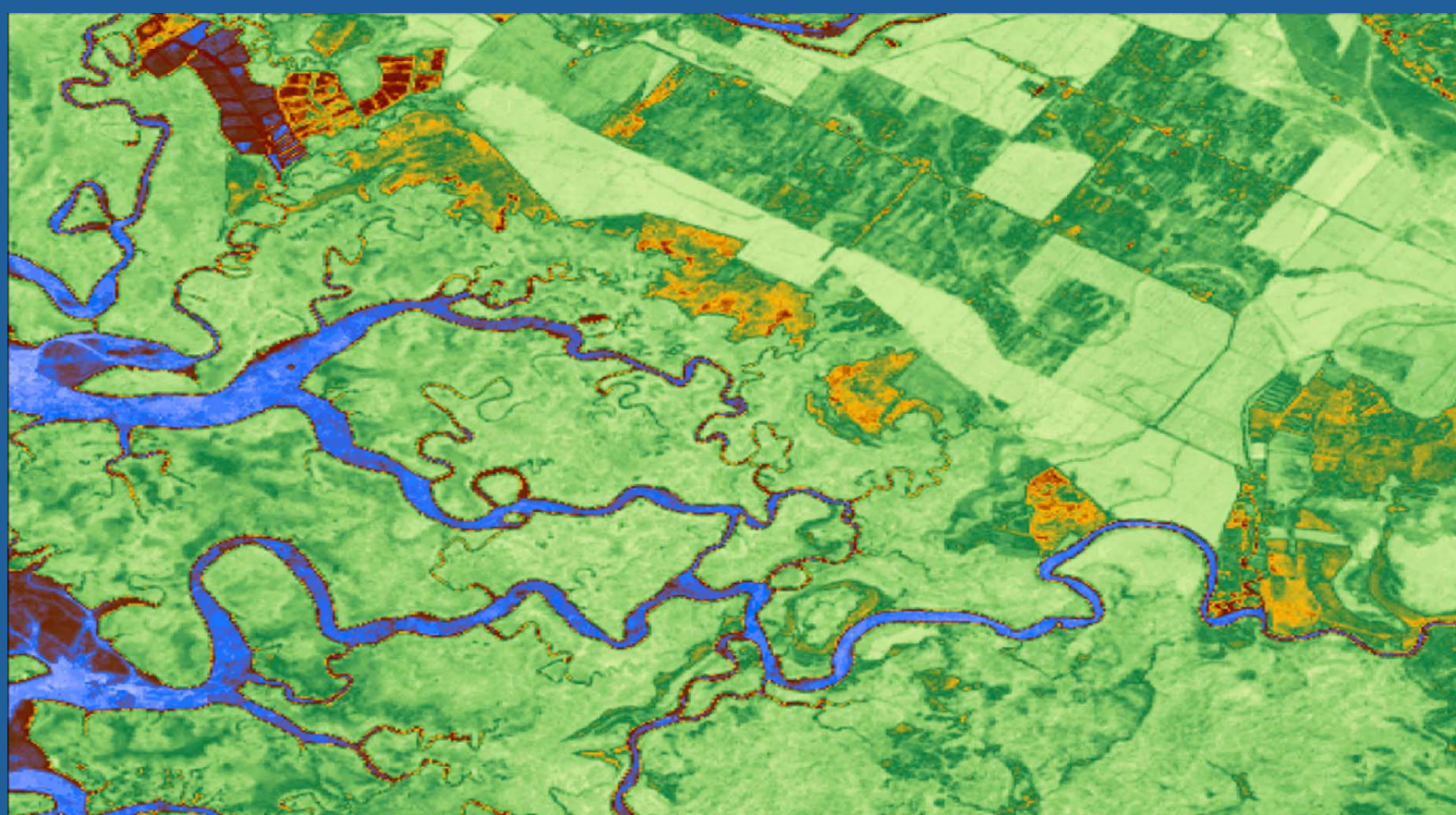


Photo Credit: NASA

**PREPARED BY:**  
Asian Institute of Technology,  
Pathum Thani, Thailand  
2024

## **Table of Contents**

<b>List of Tables.....</b>	<b>ii</b>
<b>List of Figures .....</b>	<b>iii</b>
<b>1. Introduction .....</b>	<b>1</b>
<b>2. Study Area.....</b>	<b>2</b>
<b>3. Data Acquisition and Preparation .....</b>	<b>3</b>
<b>3.1 Historical Land Cover Maps.....</b>	<b>5</b>
<b>3.2 Driving Factors.....</b>	<b>7</b>
<b>4. MOLUSCE-based Methodological Framework .....</b>	<b>13</b>
<b>4.1 Inputs .....</b>	<b>14</b>
<b>4.2 Evaluation of Correlations among Drivers.....</b>	<b>14</b>
<b>4.3 Land Cover Change Analysis and Generating Transition Matrix.....</b>	<b>15</b>
<b>4.4 Transition Potential Modelling.....</b>	<b>15</b>
<b>4.5 Cellular Automata Simulation.....</b>	<b>16</b>
<b>4.6 Model Validation.....</b>	<b>16</b>
<b>4.7 Land Cover Prediction for the Year 2030 .....</b>	<b>17</b>
<b>5. Results and Discussions.....</b>	<b>18</b>
<b>5.1 Land Cover Change Analysis between 2000 and 2020 .....</b>	<b>18</b>
<b>5.2 Comparision of Reference and Simulated Land Cover 2020.....</b>	<b>20</b>
<b>5.3 Land Cover Prediction for Year 2030 and Change Analysis.....</b>	<b>22</b>
<b>5.4 Land Cover Prediction for Years 2040 and 2050.....</b>	<b>25</b>
<b>6. Conclusion .....</b>	<b>27</b>

## List of Tables

<b>Table 1: Data Sources.....</b>	<b>4</b>
<b>Table 2: Land Cover Class Definition .....</b>	<b>5</b>
<b>Table 3: Correlations between Driving Factors.....</b>	<b>14</b>
<b>Table 4: ANN Parameters.....</b>	<b>15</b>
<b>Table 5: Land Cover Statistics between 2000 and 2010 .....</b>	<b>18</b>
<b>Table 6: Land Cover Change Statistics between 2000 and 2010.....</b>	<b>18</b>
<b>Table 7: Land Cover Change Matrix Between 2000 and 2010 .....</b>	<b>19</b>
<b>Table 8: Land Cover Change Matrix Between 2010 to 2020 .....</b>	<b>20</b>
<b>Table 9: Comparison of Reference and Simulated Land Cover 2020.....</b>	<b>21</b>
<b>Table 10: Error Matrix.....</b>	<b>22</b>
<b>Table 11: Predicted Land Cover Change Statistics between 2020 and 2030 .....</b>	<b>22</b>
<b>Table 12: Predicted Land Cover Change Matrix between 2020 to 2030 .....</b>	<b>25</b>
<b>Table 13: Predicted Land Cover Distribution for Years 2040 and 2050.....</b>	<b>25</b>

## List of Figures

<b>Figure 1: Study Area Map .....</b>	<b>2</b>
<b>Figure 2: Land Cover Map of 2000, 2010, and 2020 .....</b>	<b>6</b>
<b>Figure 3: Distance from the Road Map .....</b>	<b>7</b>
<b>Figure 4: Distance from the River Map .....</b>	<b>8</b>
<b>Figure 5: Population Density .....</b>	<b>9</b>
<b>Figure 6: Digital Elevation Model .....</b>	<b>10</b>
<b>Figure 7: Hillshade .....</b>	<b>11</b>
<b>Figure 8: Slope Map .....</b>	<b>12</b>
<b>Figure 9: MOLUSCE-based Methodological Framework .....</b>	<b>13</b>
<b>Figure 10: Artificial Neural Network Learning Curve .....</b>	<b>16</b>
<b>Figure 11: Model Validation Result .....</b>	<b>17</b>
<b>Figure 12: Reference and Simulated Land Cover 2020 .....</b>	<b>21</b>
<b>Figure 13: Predicted Land Cover 2030.....</b>	<b>23</b>
<b>Figure 14: Land Cover 2020 and Predicted Land Cover 2030.....</b>	<b>24</b>
<b>Figure 15: Predicted Land Cover 2040.....</b>	<b>26</b>
<b>Figure 16: Predicted Land Cover 2050.....</b>	<b>26</b>

## **1. Introduction**

Land cover, a fundamental component of the Earth's landscape, reflects both biotic components and the influence of natural and socio-economic factors over time (Mahmoud & Divigalpitiya, 2017; Rahman et al.). Changes in land cover are significant drivers of global environmental transformations, impacting ecosystems, infrastructure, and communities (Khan et al., 2021). Understanding and predicting land cover changes are essential for managing their effects on local environments and guiding future development. This case study report explores the prediction of future land cover changes in Ben Cat District, Vietnam, using the QGIS MOLUSCE plugin.

The QGIS MOLUSCE (Modules for Land Use Change Evaluation) plugin is a robust tool for modeling and analyzing potential future land cover scenarios based on current and historical data. This report utilizes the CA-ANN (Cellular Automata-Artificial Neural Network) method within MOLUSCE to predict land cover for Ben Cat District in the year 2030. MOLUSCE plugin is developed by Asia Air Survey and NextGIS and designed for QGIS version 2. It integrates various algorithms such as ANN, logistic regression (LR), multi-criteria evaluation (MCE), and weights of evidence (WOE), offering a comprehensive solution for simulating and validating land use changes.

This report will detail the methodologies and data sources used in the study, present the results from the MOLUSCE plugin, and assess the implications of anticipated land cover changes for the district's development. By showcasing the effectiveness of GIS-based tools in land cover prediction, this case study aims to provide valuable insights for land use planners and stakeholders, supporting informed decision-making and effective land resource management.

## 2. Study Area

The study was conducted in the Ben Cat district of Binh Duong province in southern Vietnam as shown in Figure 1, which is known for its rapid economic development and growing industrial base. The Ben Cat district is located between latitudes 11° 03" 73' and 11° 38" 94', longitudes 106° 49" 05' and 106° 72" 04'. It encompasses an area of around 580 km<sup>2</sup>. Ben Cat is also noted for its mix of urban and rural areas, with various agricultural activities alongside industrial zones. A news article published on the Nhan Dan news website indicates that Ben Cat has eight industrial parks, attracting 6,441 investment projects, including 816 foreign-invested projects with a total investment of nearly 9.8 billion USD (Minh, 2024).

The district is well-connected by roads and has seen significant infrastructure improvements in recent years. The district's topography ranges from flat plains to gently rolling hills, with elevations varying from about 5 meters to 50 meters above mean sea level (MSL). The climate is tropical, with average temperatures ranging from 25°C to 35°C. The region experiences a significant amount of rainfall, with an average annual precipitation of approximately 1800 mm (Minh, 2024).

Currently, Ben Cat district faces challenges related to rapid urban expansion and land use changes, which impact local ecosystems and infrastructure. There is increasing concern about environmental sustainability and land resource management due to these ongoing transformations.

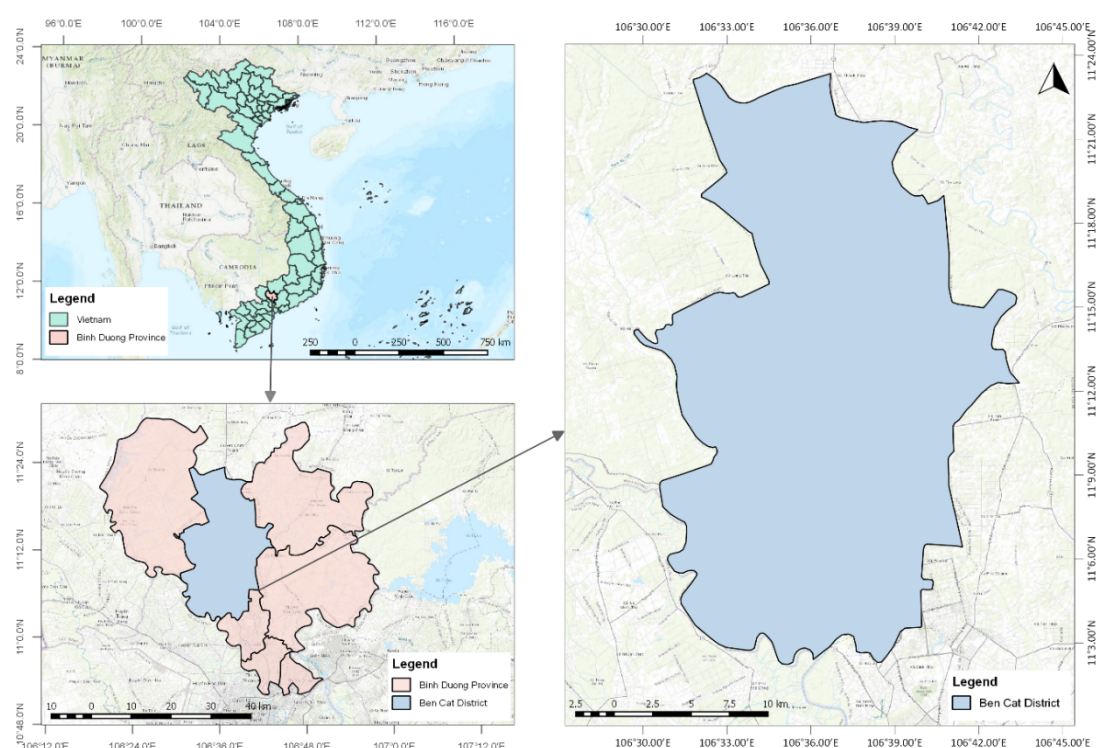


Figure 1: Study Area Map

### **3. Data Acquisition and Preparation**

Historical thematic land cover maps of the study area for 2000, 2010 and 2020 were obtained from Global Land Analysis and Discovery. The population density (2010) dataset was obtained from the Socio-economic Data and Applications Center (SEDAC), a digital elevation map (2016) and road networks (2015), both from USGS, road networks data (2015) sourced from OpenStreetMap and the river (2009) data from the Ministry of Natural Resources and Environment of Vietnam. Slope data was derived from the DEM dataset. Sources and other relevant attributes of landcover maps and driving factors are shown in Table 1.

Table 1: Data Sources

Data	Year	Source	Land cover prediction	Resolution	Data Format	Source
Historical Land Cover Maps	2000 2010 2020	Global Land Analysis and Discovery	Input maps	0.00025 Degree		<a href="https://glad.umd.edu/dataset/GLCLUC2020">https://glad.umd.edu/dataset/GLCLUC2020</a>
Population Density	2010	Socio-economic Data and Application Center (SEDAC), NASA	Spatial variable maps (Population Density)	0.00833 Degree	.tif	<a href="https://sedac.ciesin.columbia.edu/data/set/gpw-v4-population-density-rev11/data-download">https://sedac.ciesin.columbia.edu/data/set/gpw-v4-population-density-rev11/data-download</a>
DEM	2016	USGS	Spatial variable maps (DEM) Spatial variable maps (Slope)	0.00111 Degree		<a href="https://data.opendevilopmentmekong.net/en/dataset/digital-elevation-model-dem">https://data.opendevilopmentmekong.net/en/dataset/digital-elevation-model-dem</a>
Hillshade	2016	USGS	Spatial variable maps (Hillshade)	0.00111 Degree	.tif	<a href="https://data.opendevilopmentmekong.net/en/dataset/digital-elevation-model-dem">https://data.opendevilopmentmekong.net/en/dataset/digital-elevation-model-dem</a>
Road Networks	2015	OpenStreetMaps	Spatial variable maps (Distance from the road networks)			<a href="https://data.humdata.org/dataset/viet-nam-roads">https://data.humdata.org/dataset/viet-nam-roads</a>
River	2009	Department of Survey and Mapping, Ministry of Natural Resources and Environment - Vietnam	Spatial variable maps (Distance from the River)		.shp	<a href="https://data.opendevilopmentmekong.net/dataset/mng-li-thy-vn">https://data.opendevilopmentmekong.net/dataset/mng-li-thy-vn</a>

### **3.1 Historical Land Cover Maps**

The historical land cover maps of spatial resolution 0.00025 degrees were downloaded from Global Land Analysis and Discovery (GLAD). All the land cover maps were available in WGS84, geographic coordinate system and GeoTIFF (.tif format). These land cover maps primarily contain Thirteen general classes that encompass terra firma true desert, terra firma semi-arid, terra firma dense short vegetation, terra firma tree cover, wetland salt pan, wetland sparse vegetation, wetland dense short vegetation, wetland tree cover, open surface water, snow/ice, cropland, built-up and ocean. The downloaded GeoTIFF was projected into WGS UTM zone 48N, resampled into 25\*25 spatial resolution and reclassified into Four land cover classes that include forest, water bodies, built-up, and cropland as shown in Figure 2 and description of reclassified land cover classes are depicted in Table 2.

Table 2: Land Cover Class Definition

Land Cover Class	Description
Forest	Vegetation or tree cover
Cropland	Cropped area to produce annual and perennial herbaceous crops for human consumption, forage and biofuel and excludes tree crops, permanent pastures, and shifting cultivation
Built-up	Man-made land surfaces associated with infrastructure, commercial and residential land use
Water Bodies	Open surface water, rivers and other bodies of water

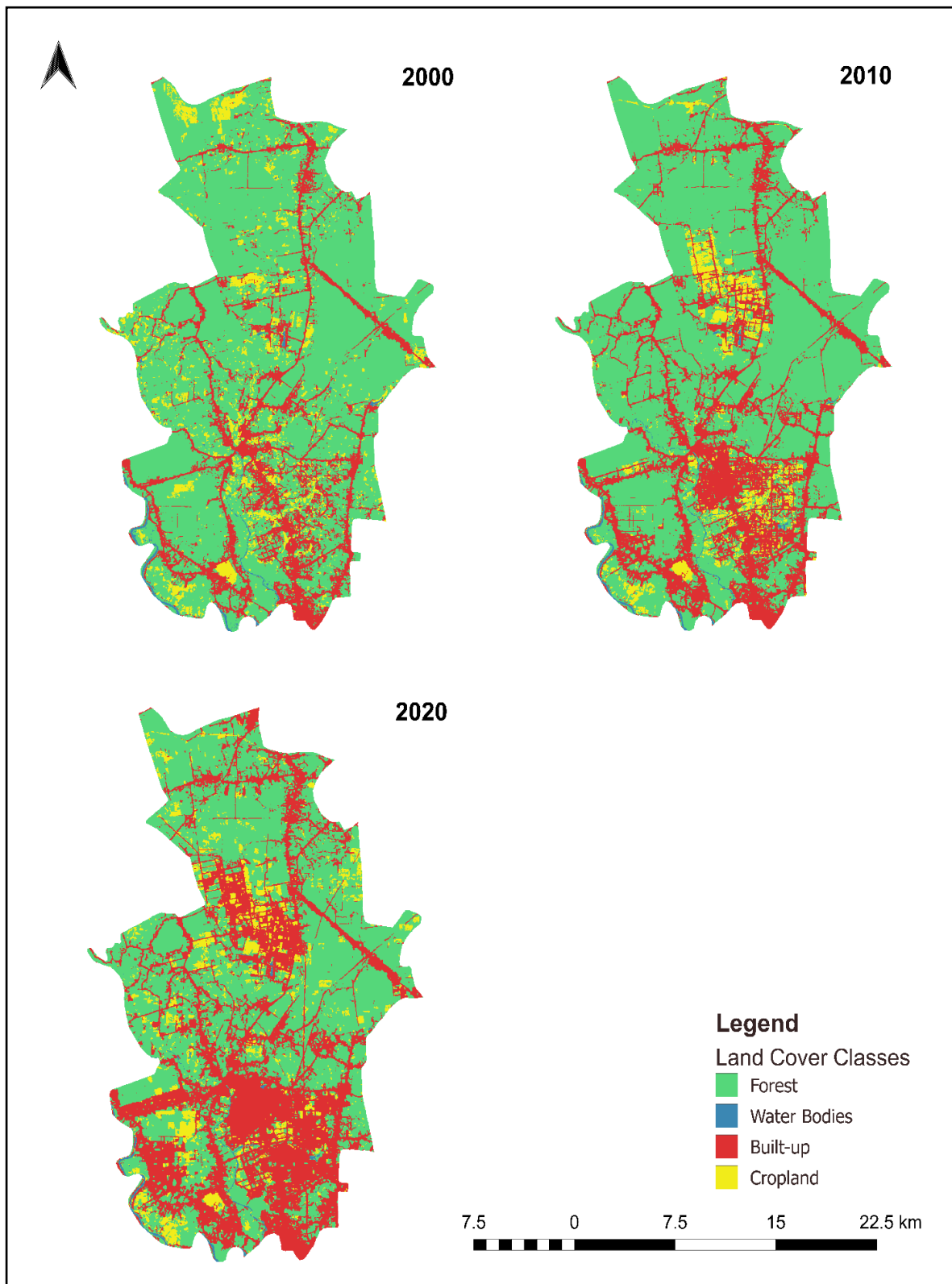


Figure 2: Land Cover Map of 2000, 2010, and 2020

### 3.2 Driving Factors

There can be a number of factors that drive land cover change. Distance from roads (Figure 3), distance from rivers (Figure 4), population density (Figure 5), DEM (Figure 6) and hillshades (Figure 7), and slope (Figure 8) were considered as the driving factors for land cover change in the study area based on data availability. Population density, DEM and hillshade datasets were initially projected into the WGS UTM zone 48N coordinate system and resampled into 25\*25 meter spatial resolution. The slope map was derived from the DEM data. Distance from the road and distance from the river data were also projected into WGS UTM zone 48N coordinate system, and Euclidean distance was calculated. Finally, all the datasets were then clipped to the same extent of the study area.

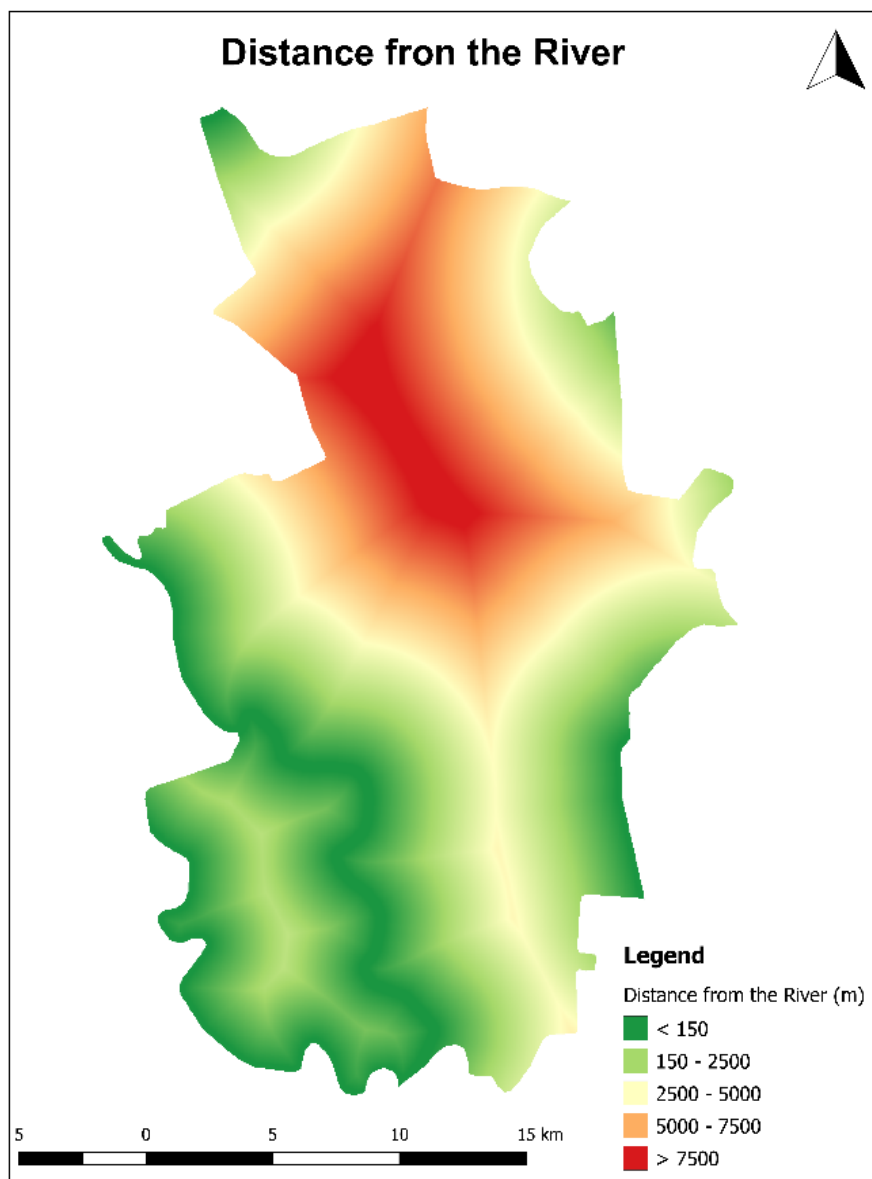


Figure 3: Distance from the Road Map

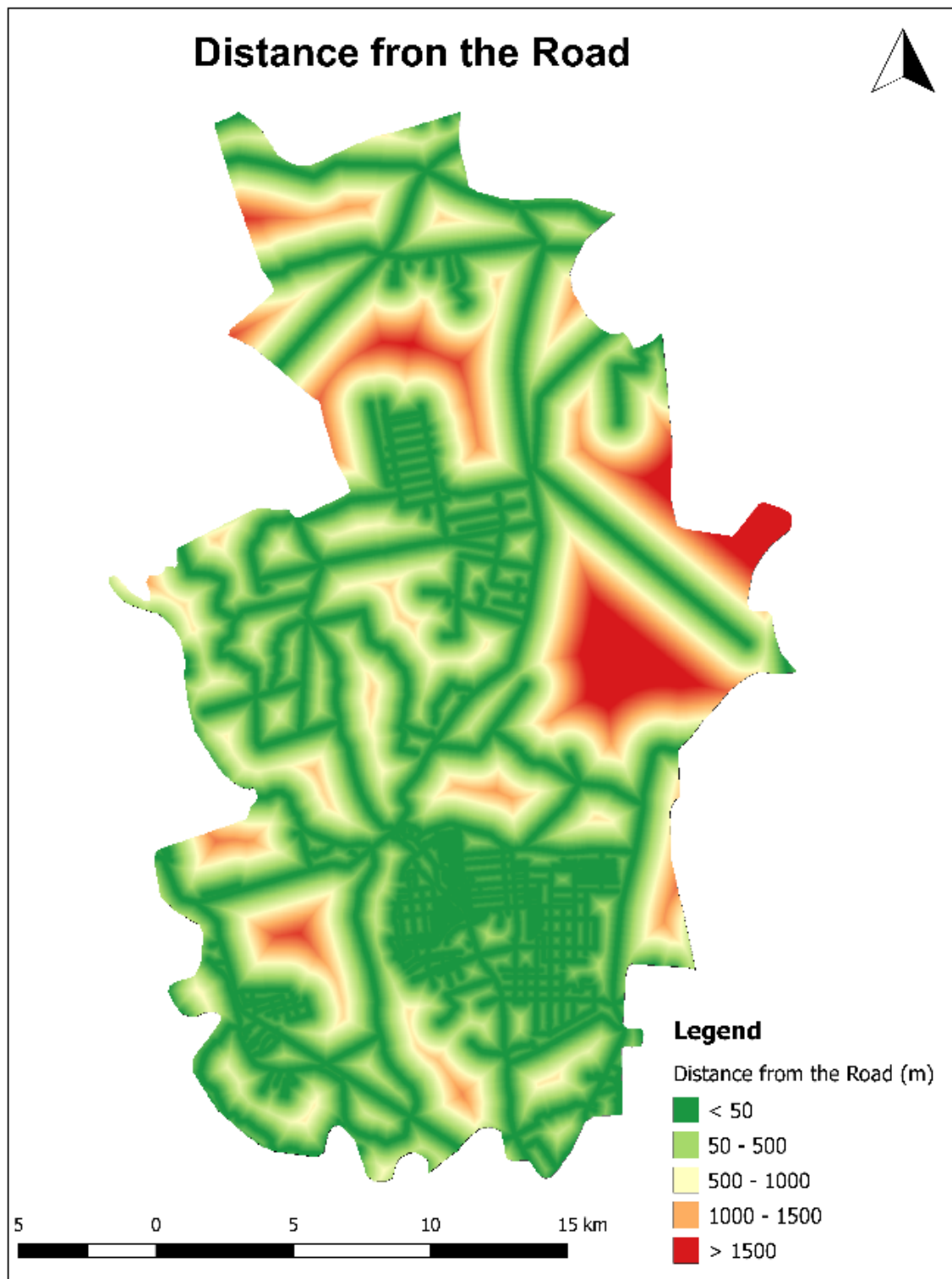


Figure 4: Distance from the River Map

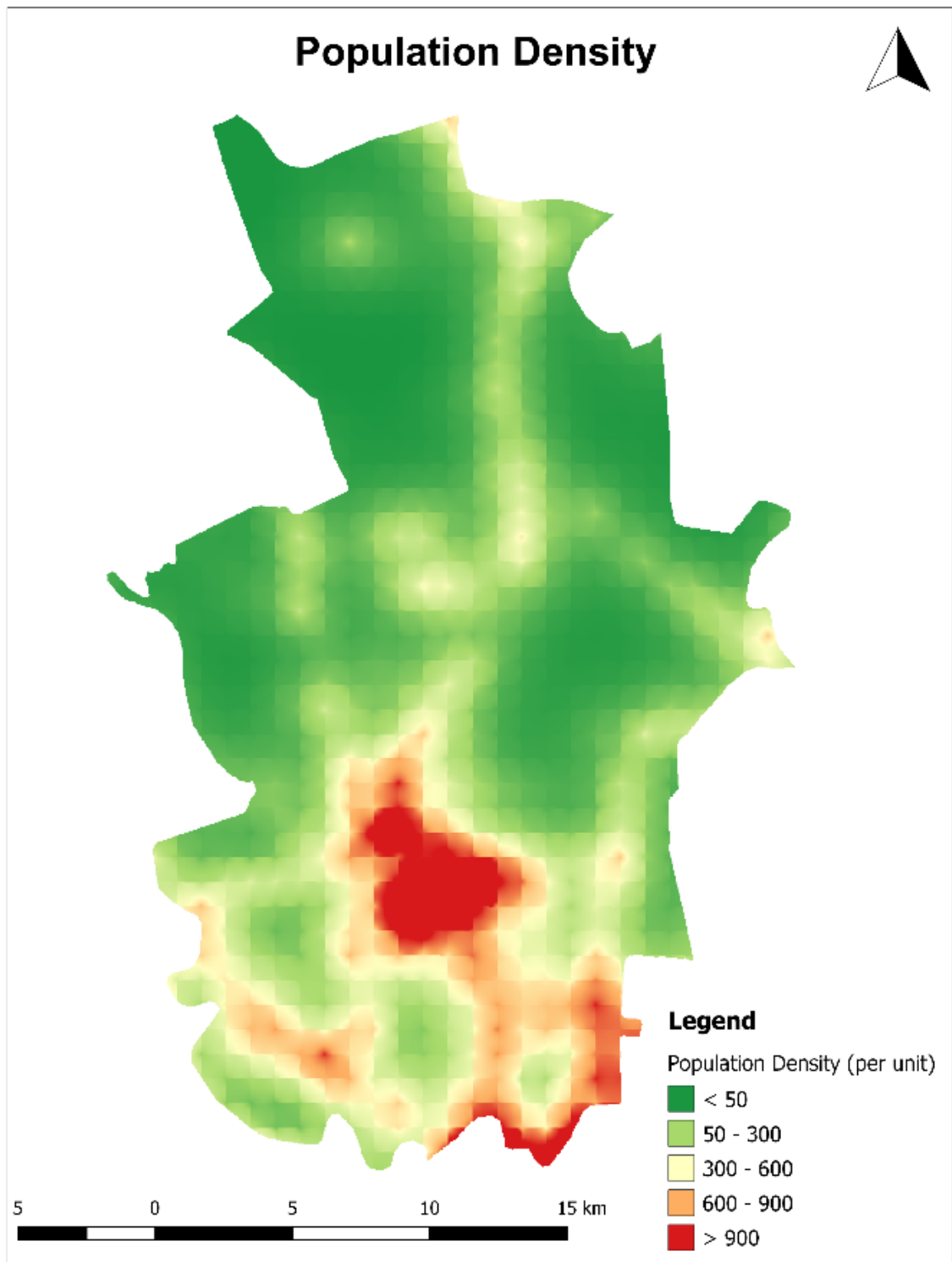


Figure 5: Population Density

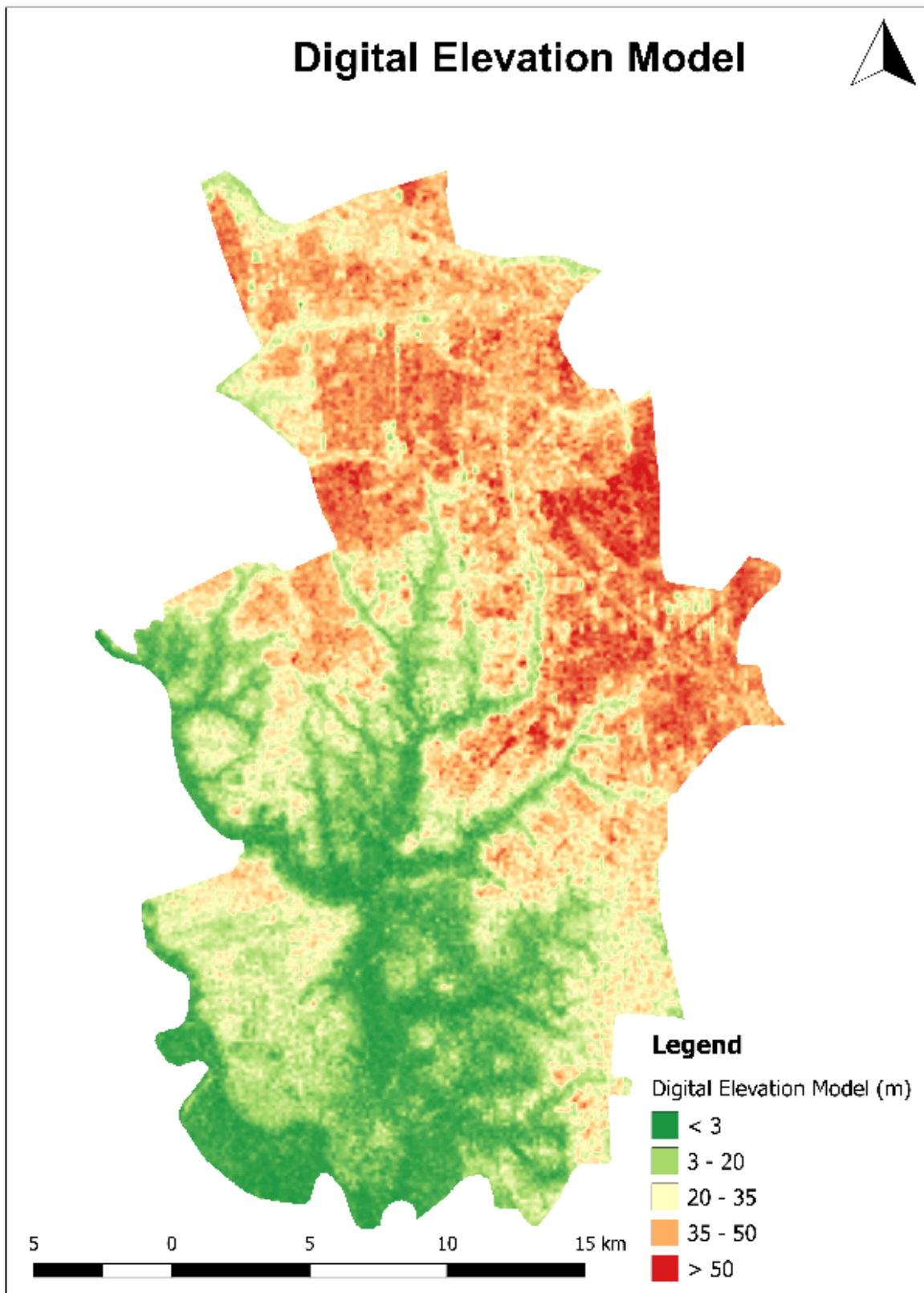


Figure 6: Digital Elevation Model

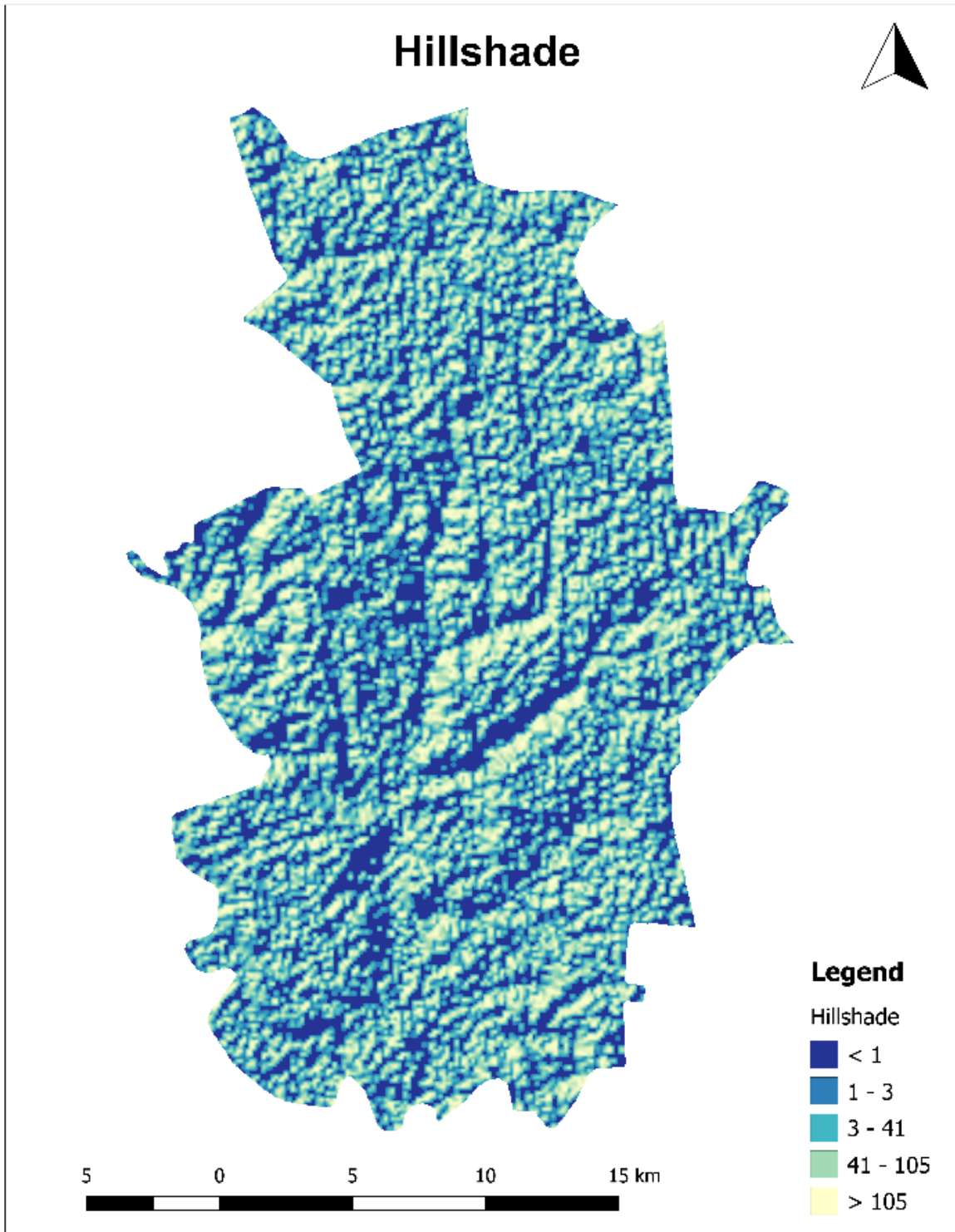


Figure 7: Hillshade

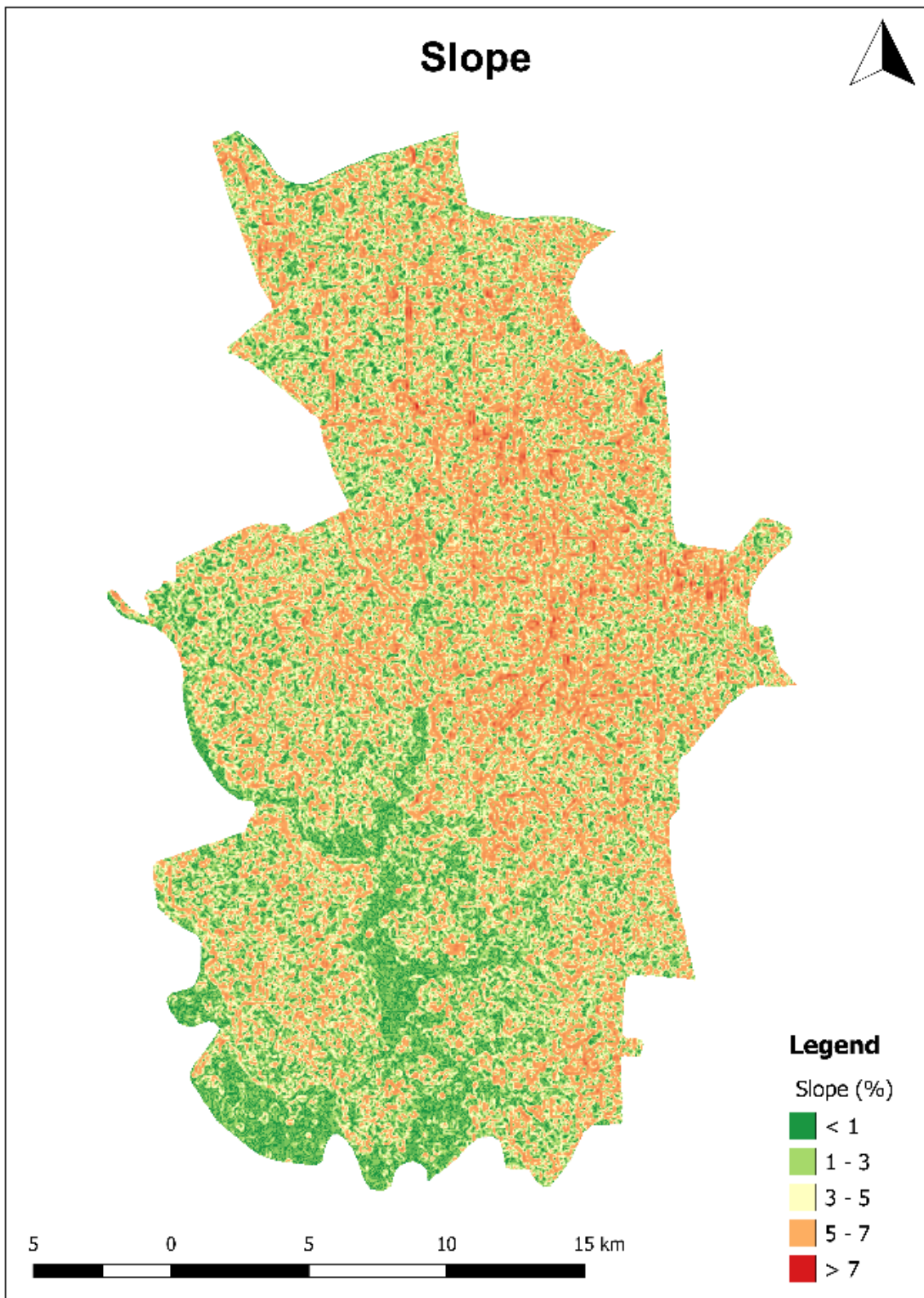


Figure 8: Slope Map

#### 4. MOLUSCE-based Methodological Framework

The overall methodology to project future land cover using MOLUSCE in QGIS is presented in Figure 9.

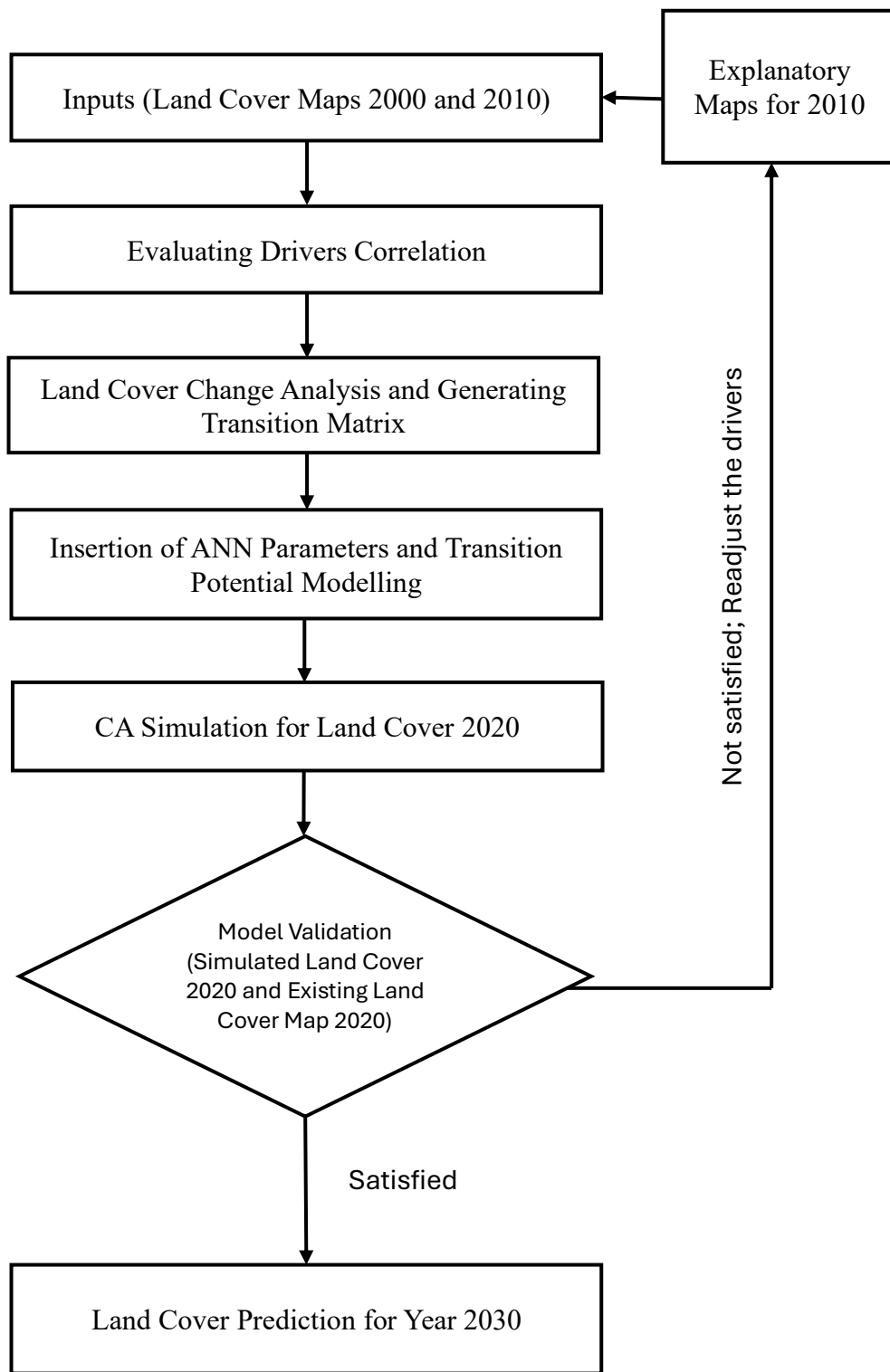


Figure 9: MOLUSCE-based Methodological Framework

## 4.1 Inputs

The initial step in MOLUSCE involves specifying the inputs that were gathered during the data preparation phase. These inputs consist of the initial land cover map 2020 and the consecutive land cover map 2010 and various driving factors that include proximity to roads and rivers, populations, digital elevation models (DEM), hillshades, and slopes.

## 4.2 Evaluation of Correlations among Drivers

There is a module in the MOLUSCE plugin for evaluating the correlation between the input driving factors, which consists of three evaluation methods - Pearson's correlation, Crammer's coefficient, and Joint Information Uncertainty. **Pearson's correlation** is useful for evaluating the linear relationships between continuous variables. **Cramér's correlation** is suitable for measuring the strength of association among categorical variables. **Joint Information Uncertainty is applicable** for capturing the amount of shared information between variables, especially for understanding dependencies in categorical data.

In our case, since all the spatial variables were continuous type, Pearson's correlation method was selected. Pearson's correlation values range from 0 to 1. If the correlation between the two drivers is more than 0.5, it is not preferred to consider during modeling and simulation. The result obtained from the correlation evaluation is demonstrated in Table 3, which indicates that each driver has a value <0.5, so all the drivers were considered for the further modelling and prediction process.

Table 3: Correlations between Driving Factors

Drivers	Hillshade	DEM	Slope	Population Density	Distance from the River	Distance from the River
Hillshade	-	-0.039	0.017	0.003	0.012	-0.014
DEM		-	0.278	-0.527	0.588	0.365
Slope			-	-0.175	0.251	0.099
Population Density				-	-0.400	-0.386
Distance from the River					-	0.105
Distance from the Road						-

### **4.3 Land Cover Change Analysis and Generating Transition Matrix**

The area changes tab under the MOLUSCE plugin was used to analyse the land cover change, generate the transition matrix and produce a change map. The land cover distribution and land cover change statistics in terms of percentage and area ( $m^2$ ) were generated for input land cover in 2000 and 2020. In addition to this, a transition matrix was generated between study periods based on the Markov chain approach. Furthermore, a land cover change map was also generated in this step.

### **4.4 Transition Potential Modelling**

MOLUSCE plugin offers four different methods to carry out transition potential modeling, including Artificial Neural Networks (ANN), Logistic Regression (LR), Multi-Criteria Evaluation (MCE), and Weights of Evidence (WOE). In this case study, transition potential modelling was carried out using the ANN method, as this is a more efficient method that is capable of handling complex modeling. Sampling and ANN parameters were altered as given in Table 4, and modeling was carried out until the satisfactory kappa(overall) was obtained in validation process (Section 4.6). After multiple trials, the ANN parameters presented in Table 4 produced the best result in this case study.

Table 4: ANN Parameters

Parameters	Value
Neighborhood	3*3
Sampling Method	Stratified
No. of Samples	30000
Learning Rate	0.001
Maximum Iterations	250
Hidden Layer	12
Momentum	0.004

Figure 10 represents the artificial neural network learning curve. Decrease in both training and validation loss to a point of stability with a minimal gap between the two final loss values can be witnessed in the learning curve which represents the well fitted model for this case study. The current validation kappa value obtained while modelling was 0.73082, exceeding 0.61, which indicates a high level of agreement. This suggests that the model is performing effectively and delivering dependable predictions.

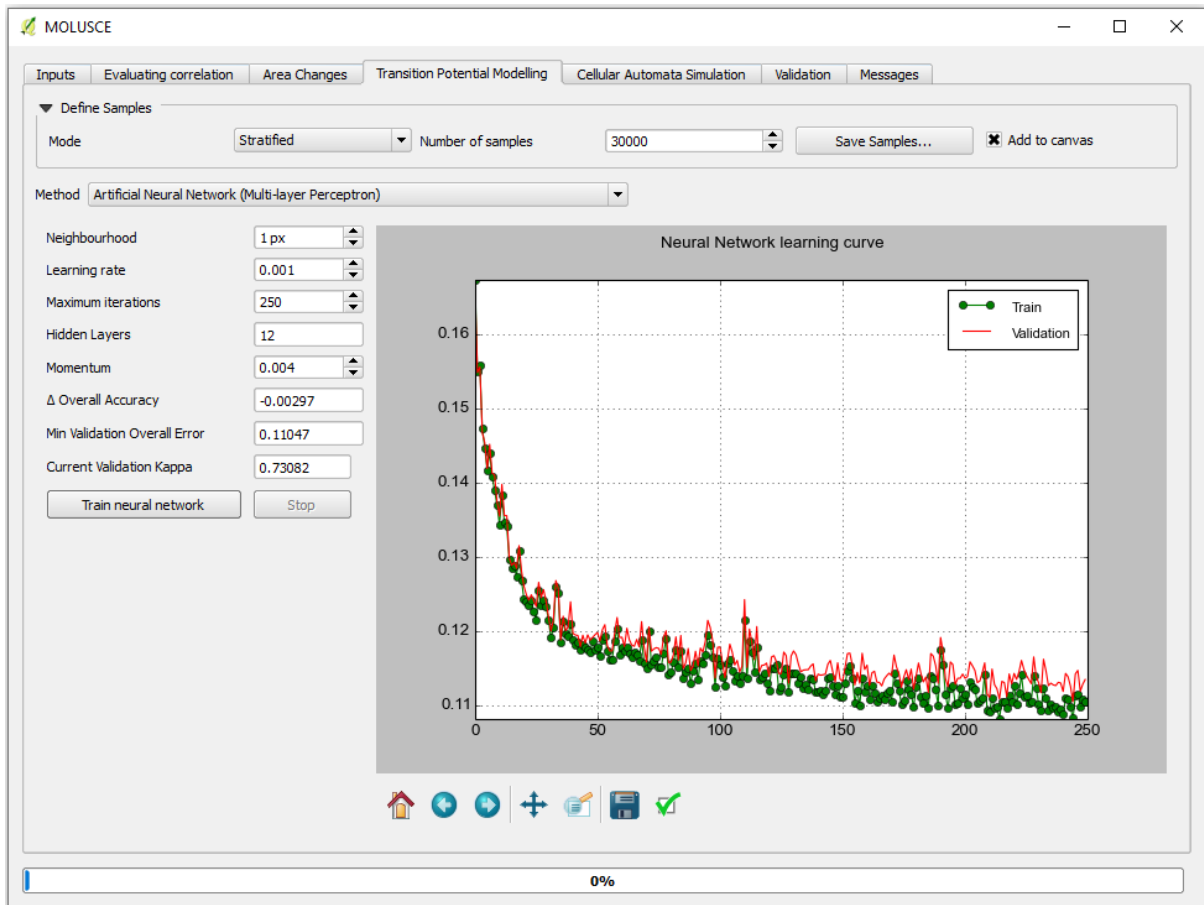


Figure 10: Artificial Neural Network Learning Curve

## 4.5 Cellular Automata Simulation

After obtaining the satisfactory transition potential modeling current validation kappa value, the land cover of the year 2020 was simulated, which is based on cellular automata simulation. The result obtained in this step is explained in the “Results and Discussion” section.

## 4.6 Model Validation

In this step, the simulated land cover map for the year 2020 was validated against the reference land cover map for the year 2020. The reliability of the model is ascertained based on the percentage of correctness and kappa statistics. The validation result can be seen in Figure 11. The values obtained for kappa local, kappa histogram, and kappa overall were 0.68, 0.92, 0.63 and an overall accuracy of 80.32% which implies the satisfactory tolerance outlined in existing studies (Kamaraj and Rangarajan (2022); Alshari and Gawali (2022); Marić et al. (2022); Uddin et al. (2023)).

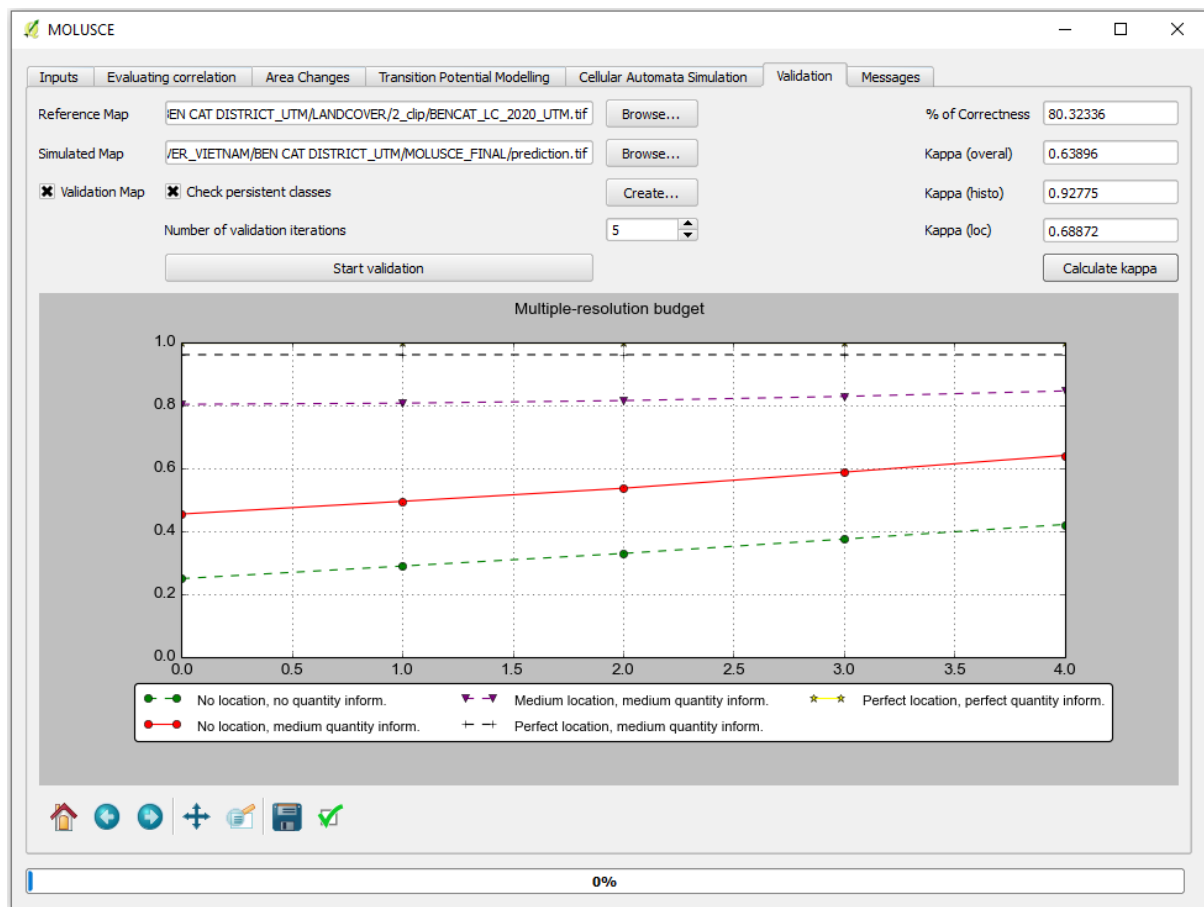


Figure 11: Model Validation Result

#### 4.7 Land Cover Prediction for the Year 2030

After obtaining satisfactory results from the model validation, inputs were updated by defining the initial land cover map 2010 and final land cover map 2020 to predict the land cover of the year 2030. In addition to this, land covers of the years 2040 and 2050 were predicted by defining iteration parameters as 2 and 3 respectively in cellular automata simulation step.

## 5. Results and Discussions

### 5.1 Land Cover Change Analysis between 2000 and 2020

Table 5 shows the land cover distribution for the years 2000, 2010, and 2020, whereas Table 6 shows the change between 2000 and 2010, 2010 and 2020, and the overall change between 2000 and 2020. The data is presented in both percentage (%) and square kilometers ( $\text{km}^2$ ) for each category.

Over the 20 years, the change analysis reveals a consistent decrease in forest land with -5.49% between 2000-2010, -13.41% between 2010-2020, and -18.9% over the decades, along with a notable expansion of built-up areas. The change in water bodies remained relatively stable throughout the study period, with cropland fluctuating and decreasing from 7.38% in 2000 to 5.12% in 2010, then rising to 7.59% by 2020. In a nutshell, these changes highlight ongoing shifts in land cover, particularly significant urban expansion and notable deforestation.

Table 5: Land Cover Statistics between 2000 and 2010

Year	2000		2010		2020	
Categories	%	$\text{km}^2$	%	$\text{km}^2$	%	$\text{km}^2$
Forest	74.31	431.18	68.82	399.33	55.41	321.52
Water Bodies	0.61	3.56	0.58	3.38	0.57	3.32
Built-up	17.7	102.71	25.48	147.86	36.43	211.38
Cropland	7.38	42.79	5.12	29.67	7.59	44.02
Total	100	580.23	100.00	580.23	100.00	580.23

Table 6: Land Cover Change Statistics between 2000 and 2010

Year	Change (2000-2010)		Change (2010-2020)		Change (2000-2020)	
Categories	%	$\text{km}^2$	%	$\text{km}^2$	%	$\text{km}^2$
Forest	-5.49	-31.86	-13.41	-77.81	-18.9	-109.66
Water Bodies	-0.03	-0.18	-0.01	-0.06	-0.04	-0.24
Built-up	7.78	45.15	10.95	63.52	18.73	108.67
Cropland	-2.26	-13.11	2.47	14.35	0.21	1.23

### a) Land Cover Change Matrix between 2000 and 2010

Table 7 shows the percentage transition of land cover classes from 2000 to 2010. The majority of forested areas (86.22%) remained unchanged, but a significant portion transitioned to built-up areas (9.35%) and cropland (4.26%). Water bodies experienced notable shifts, with 71.81% retaining their classification but 23.33% transitioning to forest, 3.43% to cropland, and 1.44% to built-up areas. The built-up class showed complete stability, with 100% of the areas remaining unchanged. In contrast, cropland was more dynamic, with only 26.14% remaining as cropland, while 62.50% converted to forest and 11.18% to built-up areas.

Table 7: Land Cover Change Matrix Between 2000 and 2010

Year	2010					
	Classes	Forest (%)	Water Bodies (%)	Built-up (%)	Cropland (%)	Total
2000	Forest	86.22	0.17	9.35	4.26	100.00
	Water Bodies	23.33	71.81	1.44	3.43	100.00
	Built-up	0.00	0.00	100.00	0.00	100.00
	Cropland	62.50	0.18	11.18	26.14	100.00

### b) Land Cover Change Matrix between 2010 and 2020

Table 8 represents land cover change matrices from 2010 to 2020. It reveals significant land cover transitions over the decade. Forested areas demonstrated relative stability, with 79.50% remaining unchanged, though 12.45% shifted to built-up areas and 7.91% to cropland. Water bodies retained a majority of their classification (80.02%), with some transitions to forest (12.36%) and other uses. Built-up areas maintained full stability, showing no change. In contrast, cropland experienced considerable transformation, with only 12.28% remaining as cropland, while a substantial portion was converted to built-up areas (46.17%) and forest (41.33%). These trends reflect ongoing urban expansion and dynamic shifts in land use, indicating a continued transformation of the landscape over the study period.

Table 8: Land Cover Change Matrix Between 2010 to 2020

Year	2020					
	Classes	Forest (%)	Water Bodies (%)	Built-up (%)	Cropland (%)	Total
2010	Forest	79.50	0.14	12.45	7.91	100.00
	Water Bodies	12.36	80.02	2.72	4.90	100.00
	Built-up	0.00	0.00	100.00	0.00	100.00
	Cropland	12.28	0.23	46.17	41.33	100.00

## 5.2 Comparision of Reference and Simulated Land Cover 2020

A comparison of the actual and simulated land cover is presented in Table 9 and Figure 12. The result shows that the model underperforms in predicting forest and built-up areas compared to water bodies and cropland. The model's underperformance in predicting forest and built-up areas can be attributed to several factors. Firstly, forests and urban areas often exhibit more complex and heterogeneous characteristics which make it challenging for the model to accurately capture their unique spectral signatures.

Additionally, the spatial distribution of forests and urban areas can be influenced by human activities, land management practices, and ecological factors, which may not be fully represented in the model's training data. In contrast, cropland tends to have more uniform and predictable patterns due to agricultural practices, making it easier for the model to learn and replicate those features.

Moreover, the resolution of the data used in the simulation may also play a role. In this case study, 25m resolution datasets were used that could obscure finer details in forest and built-up areas, leading to inaccuracies in their representation. In summary, the unique signatures and complexities associated with forest and urban environments, combined with potential limitations in training data and resolution, contribute to the model's challenges in accurately predicting these land cover types.

Table 9: Comparison of Reference and Simulated Land Cover 2020

Year	Actual Land Cover 2020		Simulated Land Cover 2020		Difference (Error)	
Categories	%	km <sup>2</sup>	%	km <sup>2</sup>	%	km <sup>2</sup>
Forest	55.41	321.52	59.31	344.15	3.9	22.63
Water Bodies	0.57	3.32	0.61	3.53	0.04	0.21
Built-up	36.43	211.38	33.25	192.91	-3.18	-18.47
Cropland	7.59	44.02	6.83	39.64	-0.76	-4.38
Total	100.00	580.23	100.00	580.23		

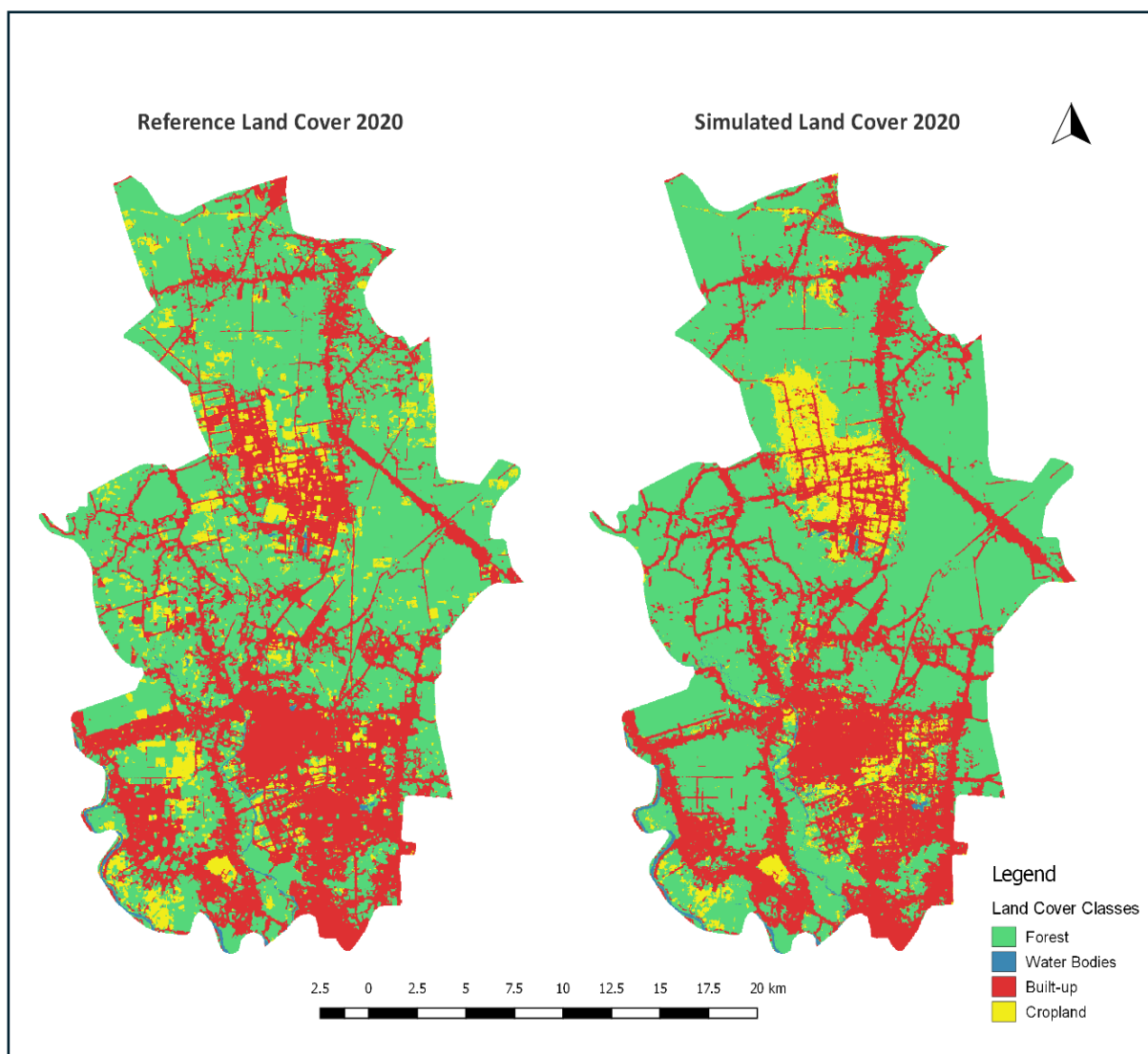


Figure 12: Reference and Simulated Land Cover 2020

Table 10 presents the error matrix from the model validation, showing that 88.56% of the forest was accurately predicted, while 22.00%, 14.06%, and 65.80% of the land were incorrectly classified as water bodies, built-up areas, and croplands, respectively. The model also correctly predicts 71.34% of water bodies, 78.89% of built-up areas, and 27.73% of croplands, with various levels of misclassification in other categories. The model notably misclassifies built-up areas as cropland in the north-central part of the study area. Overall, the accuracy of forest prediction is the highest among all land cover types at 88.56%.

Table 10: Error Matrix

Year	Simulated 2020					
	Classes	Forest (%)	Water Bodies (%)	Built-up (%)	Cropland (%)	Total
2020	Forest	88.56	0.24	7.28	3.91	100
	Water Bodies	22.00	71.34	2.84	3.82	100
	Built-up	14.06	0.08	78.89	6.97	100
	Cropland	65.80	0.45	6.03	27.73	100

### 5.3 Land Cover Prediction for Year 2030 and Change Analysis

The predicted land cover for 2030, as shown in Figure 13 and Table 11, provides significant insights into future changes. Forest areas are expected to decrease by 6.38% ( $37.03 \text{ km}^2$ ), while built-up areas are predicted to increase by 7.62% ( $44.22 \text{ km}^2$ ), reflecting significant urban expansion. Water bodies are anticipated to experience a modest net gain of 0.04% ( $0.24 \text{ km}^2$ ), and cropland is forecasted to decrease by 1.28% ( $7.44 \text{ km}^2$ ). These changes highlight the predicted shifts in land cover within the study area.

Table 11: Predicted Land Cover Change Statistics between 2020 and 2030

Year	2020		Predicted 2030		Change	
Categories	%	$\text{km}^2$	%	$\text{km}^2$	%	$\text{km}^2$
Forest	55.41	321.52	49.03	284.49	-6.38	-37.03
Water Bodies	0.57	3.32	0.61	3.56	0.04	0.24
Built-up	36.43	211.38	44.05	255.60	7.62	44.22
Cropland	7.59	44.02	6.31	36.58	-1.28	-7.44
Total	100.00	580.23	100.00	580.23		



Figure 13: Predicted Land Cover 2030

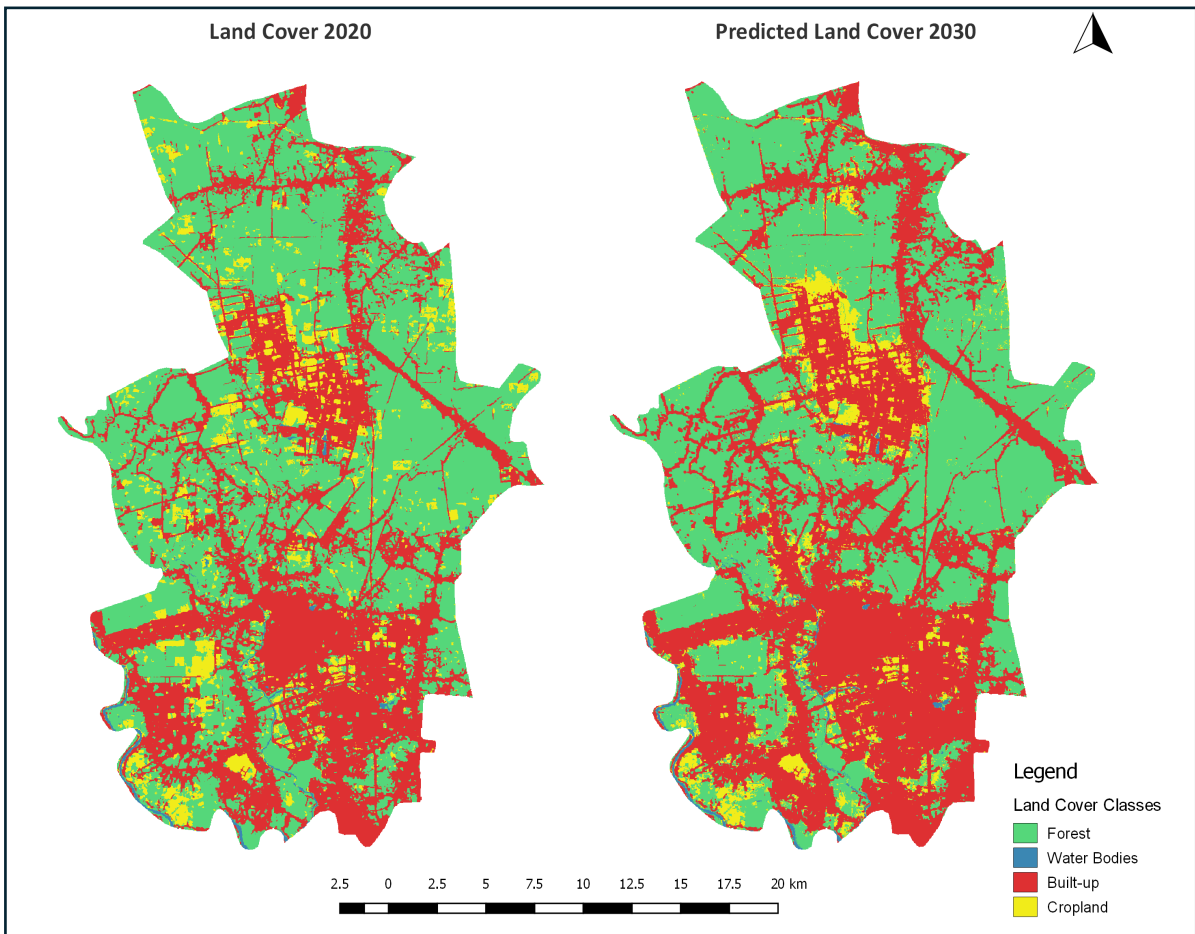


Figure 14: Land Cover 2020 and Predicted Land Cover 2030

Table 12 illustrates the predicted land cover change matrix for the period between 2020 and 2032. It shows that 78.66% of agricultural land is expected to remain unchanged by 2032. However, 3.64% of agricultural land is projected to be converted to forest, 2.00% to barren land, and 15.70% to built-up areas. Moreover, forest land is expected to remain stable for 82.37%, while 25.53% of barren land and 73.62% of built-up areas will also remain unchanged by 2032. In contrast, 15.16% of forest land is forecasted to transition to agriculture, 0.29% to barren land, and 2.18% to built-up areas. Additionally, 37.24% of barren land is projected to change to agriculture, 2.88% to forest, and 25.53% to built-up areas. Similarly, 17.80%, 6.08%, and 2.51% of forest land are anticipated to be converted to agriculture, forest, and barren land, respectively.

Table 12: Predicted Land Cover Change Matrix between 2020 to 2030

Year	2030					
	Classes	Forest (%)	Water Bodies (%)	Built-up (%)	Cropland (%)	Total
2020	Forest	81.79	0.23	12.28	5.70	100
	Water Bodies	12.61	82.52	1.49	3.39	100
	Built-up	0.05	0.00	99.95	0.00	100
	Cropland	47.73	0.17	10.92	41.18	100

#### 5.4 Land Cover Prediction for Years 2040 and 2050

Using the same input land cover map of 2010 as an initial and 2020 as a final and setting the iteration parameters 2 and 3, the land cover map for 2040 (Figure 15) and 2050 (Figure 16) was predicted. Table 13 represents the predicted land cover distribution for the years 2040 and 2050.

Table 13: Predicted Land Cover Distribution for Years 2040 and 2050

Year	2040		2050		
	Categories	%	km <sup>2</sup>	%	km <sup>2</sup>
Forest	44.67	259.18	41.11	238.55	
Water Bodies	0.66	3.81	0.67	3.89	
Built-up	48.94	283.97	52.76	306.13	
Cropland	5.73	33.16	5.46	31.66	
Total	100.00	580.23	100.00	580.23	

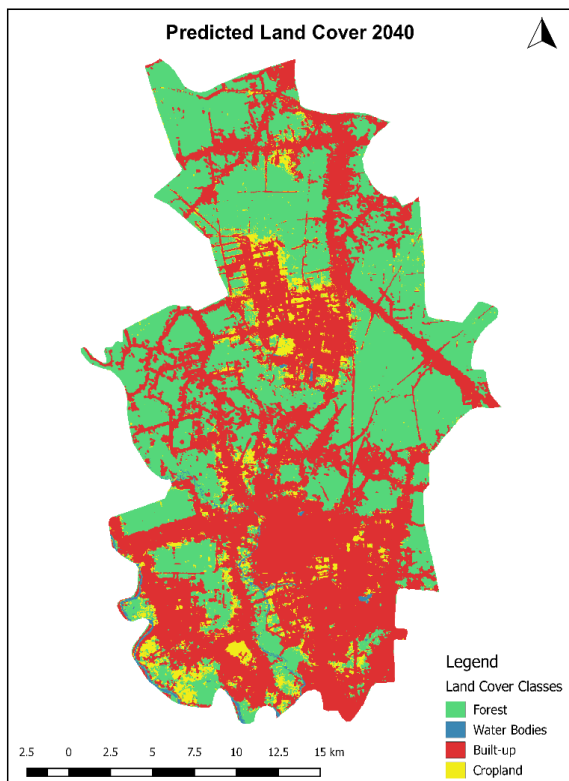


Figure 15: Predicted Land Cover 2040

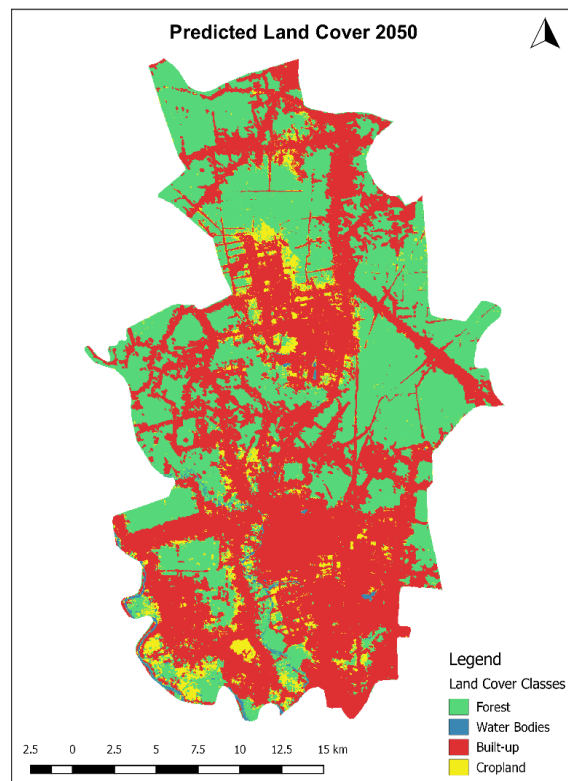


Figure 16: Predicted Land Cover 2050

## **6. Conclusion**

In this study, the future land cover of the Ben Cat district of Binh Duong province in Vietnam was predicted using the Cellular Automata-Artificial Neural Network (CA-ANN) model, implemented through the MOLUSCE plugin in QGIS. This study underscores the usefulness of the CA-ANN model in providing insights into land cover dynamics, allowing for informed decision-making and strategic planning. However, the limitations are notable; the exclusion of key factors such as development policies and climate conditions may lead to simplified predictions. The results reveal that Ben Cat is experiencing significant urban expansion, leading to the degradation of forest land. This trend highlights the urgent need for relevant authorities to implement proactive land management strategies to address the potential negative impacts on green forest coverage and agricultural productivity, which are vital for ensuring regional food security. The study focused on four primary land cover classes - forests, water bodies, built-up areas, and agriculture. While the prediction was based on physical and socio-economic drivers, it's important to acknowledge that other driving factors, including development policies, migration, immigration, and climate conditions, were not incorporated but could significantly affect land cover patterns. The study also suggests that integrating agricultural and urban development policies could enhance more sustainable urbanization practices, balancing growth with environmental preservation. Given the limitations of the current study, research should aim to include a wide range of land cover classes, additional driving factors, and higher-resolution land cover maps. This would enhance the accuracy of the predictions, providing a more comprehensive understanding of land cover dynamics and informing more effective land management planning.

## REFERENCES

- Khan, Z., Saeed, A., & Bazai, M. (2021). Land use/land cover change detection and prediction using the CA-Markov model: A case study of Quetta city, Pakistan. 2, 164-182.
- Mahmoud, H., & Divigalpitiya, P. (2017). Modeling Future Land Use and Land-Cover Change in the Asyut Region Using Markov Chains and Cellular Automata. In A. Bisello, D. Vettorato, R. Stephens, & P. Elisei (Eds.), Smart and Sustainable Planning for Cities and Regions: Results of SSPCR 2015 (pp. 99-112). Springer International Publishing. [https://doi.org/10.1007/978-3-319-44899-2\\_7](https://doi.org/10.1007/978-3-319-44899-2_7)
- Minh, L. Q. (2024). Binh Duong Province announces the establishment of Ben Cat City. *Nahn Dan*.
- Rahman, M. T. U., Tabassum, F., Rasheduzzaman, M., Saba, H., Sarkar, L., Ferdous, J., Uddin, S. Z., & Zahedul Islam, A. Z. M. Temporal dynamics of land use/land cover change and its prediction using CA-ANN model for southwestern coastal Bangladesh. (1573-2959 (Electronic)).
- Alshari, E. A., & Gawali, B. W. (2022). Modeling Land Use Change in Sana'a City of Yemen with MOLUSCE. *Journal of Sensors*, 2022, 7419031. <https://doi.org/10.1155/2022/7419031>
- Marić, I., Pandža, L., Faričić, J., Šiljeg, A., Domazetović, F., & Marelić, T. (2022). Long-Term Assessment of Spatio-Temporal Landuse/Landcover Changes (LUCCs) of Ošljak Island (Croatia) Using Multi-Temporal Data—Invasion of Aleppo Pine. *Land*, 11(5). <https://doi.org/10.3390/land11050620>
- Uddin, M. S., Mahalder, B., & Mahalder, D. (2023). Assessment of Land Use Land Cover Changes and Future Predictions Using CA-ANN Simulation for Gazipur City Corporation, Bangladesh. *Sustainability*, 15(16). <https://doi.org/10.3390/su151612329>
- Kamaraj, M., & Rangarajan, S. (2022). Predicting the Future Land Use and Land Cover Changes for Bhavani Basin, Tamil Nadu, India, Using QGIS MOLUSCE Plugin. *Environmental Science and Pollution Research*, 29(57), 86337-86348. <https://doi.org/10.1007/s11356-021-17904-6>